



## Cooling power of sea breezes and its inland penetration in dry-summer Adelaide, Australia

Yifei Zhou<sup>\*</sup>, Huade Guan<sup>\*</sup>, Saeedeh Gharib, Okke Batelaan, Craig T. Simmons

National Centre for Groundwater Research and Training & College of Science and Engineering, Flinders University, Bedford Park, South Australia, Australia



### ABSTRACT

Extreme high-temperature events pose a threat to human beings on Earth. In coastal cities, the sea breeze is widely known as a prevailing wind that can cool the near-surface air. However, the cumulative cooling effect and its attenuation process during the sea breeze penetration have not been well investigated. In this study, we analyze sea breeze cooling capacity (SBCC) and propose a new method in estimating the penetration distance of sea breeze cooling in metropolitan Adelaide during summer using data from the Adelaide urban heat island monitoring network. The results show that during a sea breeze day, wind direction rapidly changes from southeast to southwest in the morning, and it gradually returns to southeast in the afternoon. It takes 67 min on average for the sea breeze cooling fronts to penetrate inside metropolitan Adelaide. The SBCC value is 21.3 °C h per event averaged spatially in Adelaide summer. During the penetration process, the SBCC values decrease at a rate of 0.7 and 0.9 °C h per kilometer from coast to inland on an average sea breeze day and a hot sea breeze day, respectively. Correspondingly, the mean cooling penetration distances are 42 and 29 km along the prevailing wind path. A multiple linear regression analysis indicates that the distance from the coast and elevation at the onshore point together explain 88% of the spatial variability of the temporally average SBCC in the study area. The spatial pattern and penetration distance of the cumulative sea breeze cooling effect contribute to a better understanding of this common cooling source for heat mitigation in coastal cities where a large number of people reside.

### 1. Introduction

Different thermal properties between land and sea lead to a contrast of air temperature for both sides. This phenomenon can generate a low-level atmospheric inland or ocean-directed airflow, generally described as a sea-land breeze. In the nighttime when the land cools faster than the nearby sea, wind blows from the land to the sea forming the land breeze. During the daytime when air temperature over the land is higher, wind direction reverses, forming the sea breeze. The sea-land breeze is a mesoscale atmospheric phenomenon recurring on a diurnal cycle along about 2/3 of coasts in the world, especially in tropical and subtropical zones (Pattiaratchi and Gould, 1997). It has attracted high attention for highly populated coastal areas, as it influences the thermodynamic structure of air and changes the atmospheric environment by dispersion effect inside the boundary layer (Yamamoto and Ishikawa, 2020; Zhang et al., 2019).

Multiple studies have analyzed the roles of different temporal and spatial variables in explaining the intensity, coverage and key time points of sea-land breeze events (Chen et al., 2011; Meir et al., 2013; Arrillaga et al., 2016). These influencing factors can be generally classified into meteorological variables, local geographical variables and anthropogenic factors. The time-varying meteorological variables

mainly consist of cloud fraction, atmospheric stability, direction and intensity of synoptic wind. For example, cloudiness in the sky can lead to a relatively cool land surface, which is unfavorable for the formation of a sea breeze at daytime (Kala et al., 2010). As for the synoptic background, Azorin-Molina and Chen (2009) found that offshore synoptic flows contributed to a delay of sea breeze arrival on land while onshore synoptic flows had an opposite effect. In Yokohama, Japan, patterns with southwestern synoptic wind were revealed to have stronger effects on air temperature compared to other background patterns in sea breeze events (Sasaki et al., 2018). Other characteristics of sea breezes, such as maximum wind speed, height of sea breeze front, and shape of sea breeze circulation have also been found to be significantly influenced by synoptic flows (Miller et al., 2003; Poljak et al., 2014). Generally, local geographical variables, such as land use pattern, terrain and shape of the coast are time-invariant with respect to atmospheric processes. The location of the Durance Valley (Marseille area, France) was reported to impair sea-land breeze circulation by decreasing the temperature gradient along the wind path (Bastin et al., 2005). In addition, curvature of shoreline has been found to determine convergence or divergence of sea breezes according to a study in Israel (Neumann, 1951). Anthropogenic factors of sea breezes include aerosol particles, urban structure, and urban heat island, etc. For example, emission of aerosol particles can

\* Corresponding author at: National Centre for Groundwater Research and Training, College of Science and Engineering, Flinders University, Australia.  
E-mail address: [huade.guan@flinders.edu.au](mailto:huade.guan@flinders.edu.au) (H. Guan).

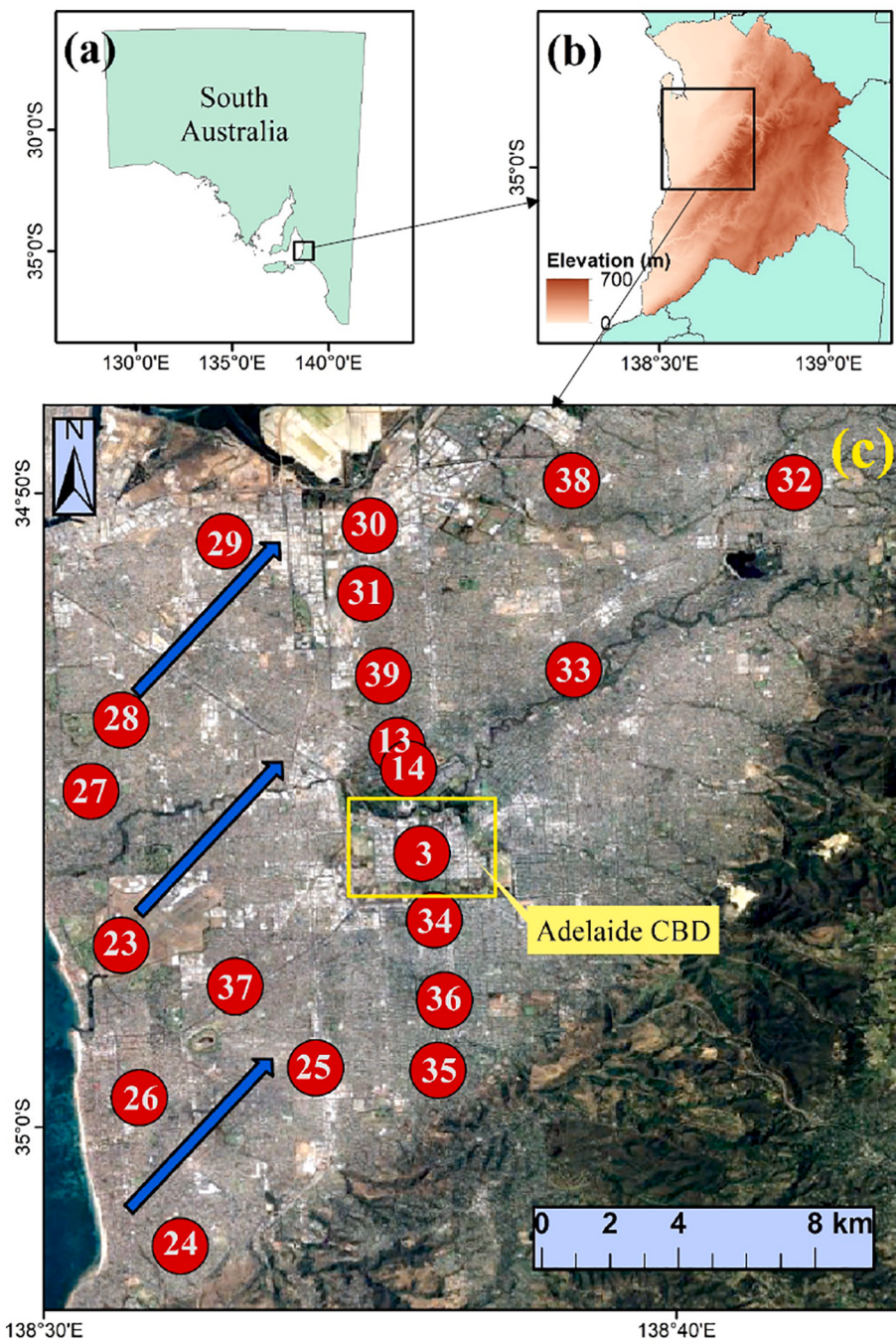


**Fig. 1.** Maps showing the location of metropolitan Adelaide and the distribution of temperature sensors in the study area (circles). (a) Map of south Australia; (b) Topography of metropolitan Adelaide area; (c) Distribution of temperature sensors. The blue arrows represent the mean prevailing wind direction (south-westerly) during sea breezes. The topography map is derived from DEM data.

decrease solar radiation and thus reduce the magnitude of wind speed during sea breezes in coastal areas (Shen and Zhao, 2020). In Sydney, observations have found a positive relationship between sky view factor and wind speed during the sea breeze, while wind can be enhanced in street canyons (He et al., 2020).

For coastal cities, the urban environment can significantly interact with the sea-breeze circulation. In Tokyo, the urban heat island circulation has been found to delay the arrival of inland propagation of sea breezes and contribute to an upward convergence at the sea breeze front due to wind shear (Ado, 1992). In addition, increased surface roughness caused by urbanization could contribute to the weakening of sea breezes which has been found in cities such as Athens and Shanghai (Dandou

et al., 2009; Shen et al., 2019). On the other hand, in large cities at a distance from the coast, such as São Paulo, sea breezes can be strengthened by the existence of urban heat island circulation resulting from a strong convergence zone in the city center (Freitas et al., 2007). The sea breeze onset time could be earlier if there is an enhanced urban heat island effect in the morning (Khan and Simpson, 2001). This interaction can also change the urban climate inside the city. The height of urban boundary layer has been found to be reduced due to the passage of a sea breeze front (Ribeiro et al., 2018). Ohashi and Kida (2002) revealed the shift in the center of urban heat island circulation towards the inland suburbs during sea breeze events. More importantly, sea breezes have been found to mitigate urban heat island in many cities

globally (Guan et al., 2016; Kim and Baik, 2004; He, 2018). There is no doubt that sea breeze cooling can improve human's comfort level and is beneficial in reducing energy consumption during heatwave days (Lopes et al., 2011).

The last decades have witnessed noteworthy increases in intensity and duration of heatwave events globally (Coulomou and Rahmstorf, 2012; Wang and Zhu, 2020). For example, Trewin and Vermont (2010) revealed that there were positive trends for both daily maximum and minimum temperature from 1957 to 2009 in Australia. They have resulted in some adverse consequences such as increasing mortality and excessive energy consumption in summer (Lapola et al., 2019; Smoyer-Tomic et al., 2003). The sea breeze could be a potential cooling source for coastal cities where a large number of people reside. It can be helpful for mitigating the unfavorable aspects of heatwaves. Some studies have already explored the characteristics of sea breezes and their impacts on air temperature based on observations and numerical simulations (Furberg et al., 2002; Huang et al., 2016; Naor et al., 2017). Particularly investigated are the spatial patterns of air temperature during sea breeze events. For example, based on a high-density temperature observation network, Yamato et al. (2017) noted a significantly lower air temperature in central Tokyo than that in the leeward suburbs during a sea breeze. However, no study has examined the cumulative cooling effect of sea breezes inside the whole metropolitan area and estimated its penetration distance, which is the focus of this study based on Adelaide, a coastal city in South Australia.

Recently, Zhou et al. (2019) proposed the metric of sea breeze cooling capacity (SBCC) for quantifying the cumulative cooling effect of sea breezes. They analyzed its temporal and spatial patterns for the Central Business District (CBD) of Adelaide, Australia. In this study, we continue to use this proposed metric to perform a quantitative analysis of sea breeze cooling in metropolitan Adelaide and propose a new method to estimate its inland penetration distance. Additionally, the basic climatological characteristics of sea breezes are investigated because they are helpful in understanding how sea breeze cooling forms and varies.

The objectives of this study are:

- (1) To determine the major climatological characteristics of sea breezes in the coastal area of Adelaide during summer.
- (2) To illustrate, quantify and attribute the spatial patterns of sea breeze cooling during all sea breeze days and hot sea breeze days and explain their difference.
- (3) To estimate the penetration distance of sea breeze cooling in the Adelaide metropolitan area.

## 2. Data and methods

### 2.1. Study area

Located on the south coast of the Australian continent, metropolitan Adelaide is built on the Adelaide Plains bounded by the Mount Lofty Ranges to the east (Fig. 1). Adelaide has a temperate Mediterranean climate with scorching summer and mild winter. The prevailing winds in winter are the large-scale synoptic flows that mostly come from north, while in summer southerly winds dominate (Masouleh, 2015). A clear temperature gradient from coast to inland has been found in summer daytime and this phenomenon is supposed to be generated from prevailing sea breezes (Guan et al., 2016). This region occasionally suffers from excessive hot weather with temperature up to 46 °C caused by anticyclone systems centered within the range of 35° – 40°S during summer days. It is predicted that the annual mean temperature will increase up to more than 3 °C by 2070 in Adelaide (Suppiah et al., 2006) and this can inevitably worsen the living conditions of local residents. Thus, optimizing cooling sources for heat mitigation will become increasingly important in Adelaide. Located in the center of the metropolitan Adelaide, the Adelaide CBD is an area of <10 km<sup>2</sup> covered by a

**Table 1**

Information of temperature monitoring stations (4 m above ground) in metropolitan Adelaide, including names and geographic coordinates.

ID	Location	Latitude	Longitude
3	Victoria Square	34°55'41"S	138°35'58"E
13	Park near Adelaide Aquatic Centre	34°53'59"S	138°35'35"E
14	Corner O'Connell/Tynte	34°54'21"S	138°35'45"E
23	Adelaide Airport	34°57'8"S	138°31'13"E
24	Eyre Street	35°1'52"S	138°32'9"E
25	Talisman Avenue	34°59'3"S	138°34'17"E
26	Harding Street	34°59'32"S	138°31'30"E
27	Kent Avenue	34°54'42"S	138°30'44"E
28	Foot Avenue	34°53'35"S	138°31'13"E
29	Francis Road	34°50'45"S	138°32'51"E
30	Duncan Road	34°50'30"S	138°35'9"E
31	Northcote Street	34°51'35"S	138°35'5"E
32	Gorman Street	34°49'49"S	138°41'51"E
33	Clarence Avenue	34°52'47"S	138°38'22"E
34	Roberts Street	34°56'44"S	138°36'10"E
35	Mitcham Avenue	34°59'6"S	138°36'13"E
36	Clifton Street	34°58'0"S	138°36'20"E
37	Colarado Avenue	34°57'47"S	138°33'1"E
38	Winara Drive	34°49'47"S	138°38'20"E
39	Beatrice Road	34°52'53"S	138°35'21"E

mix of high-rise and low-rise buildings with maximum height up to 130 m. The parkland belt around the Adelaide CBD exhibits lower temperatures than the built-up area (Guan et al., 2015; Clay and Guan, 2020). Green roofs have also been found to cool the nearby area in central Adelaide (Razzaghmanesh et al., 2016). However, these cooling sources take effects at a limited spatial scale with a cost of water, electricity and maintenance. The sea breeze, in contrast, can influence a much larger area.

### 2.2. Data

In this study, we focus on summer days for two reasons: (1) A previous study demonstrated that sea breezes are most frequent during this season in Adelaide (Masouleh, 2015); (2) sea breeze cooling is of most concern during summer days, especially in days with heatwaves. According to the monthly mean temperatures, summer season is defined as December, January, February and March in Adelaide, a city in the southern hemisphere. Therefore, these months are considered in our analysis. Altogether, 364 summer days during December 2010 – March 2013 are selected.

The selection of sea breeze days is performed using a combination of observed data and retrieved data. The observed data are from Adelaide Airport weather station (34.95°S, 138.52°E), which is located only 1.5 km eastwards from the coast with measurement heights being 1.2 m for the temperature sensor, 6.2 m for the barometer and 10 m for the anemometer. The surrounding area of this station is flat without high-rise buildings, so the information provided by this station is supposed to represent the local weather condition. In this study, meteorological data from this station are obtained from Bureau of Meteorology, Australia (<http://www.bom.gov.au/climate/data/>). For the sea breeze identification, three variables with 10-min temporal resolution are used: specific humidity (g/kg), air temperature (°C), and wind direction (°). In addition, data of sea surface temperature (SST) and land surface temperature (LST) are adopted to derive the temperature difference between land and sea, which is an additional criterion in the identification of sea breeze days. Daily SST data near the Adelaide coast are obtained from NOAA/NCEI (<https://www.ncdc.noaa.gov/oisst>), while daily LST data are derived from MODIS/Aqua measurements (<https://search.earthdata.nasa.gov/search>). For simplicity, time interpreted below is local standard time in Adelaide (GMT +9:30).

We use data from the Adelaide urban heat island monitoring network to quantify the cooling effect during sea breeze events. This network was composed of multiple Maxim Thermochron Ibutton Sensors distributed

relatively uniform across metropolitan Adelaide. These sensors were located away from building walls where strong convections and wind shears are frequent. Under this condition, the local effects caused by small-scale barriers such as buildings and trees would be eliminated to the maximum extent. The Adelaide urban heat island monitoring network measured data every 30 min at the height of 4 m from 2010 to 2013. In total, 39 sensors were installed of which 22 were inside the Adelaide CBD and northern Adelaide (Fig. 1, Table 1). In this study, we exclude most of the sites in the Adelaide CBD and northern Adelaide to eliminate the effects of high-rise buildings to the maximum extent and therefore the selected sites distribute relatively uniformly over metropolitan Adelaide. Overall, data from 20 sites are used. Site 3 is selected to represent the weather condition in the Adelaide CBD as this site is in an open area with less interference of high-rise buildings compared to other sites. The SBCC at this site is close to the average over the surrounding area (Zhou et al., 2019).

In addition, we have used DEM (Digital Elevation Model) data in metropolitan Adelaide with 30-m resolution to calculate relevant geographic quantities such as the distance from the coast. This DEM data is obtained from Department for Environment and Water, South Australia. NCEP/NCAR reanalysis data with the spatial resolution being  $2.5^\circ \times 2.5^\circ$  have also been used for the analysis of synoptic background during sea breeze days (<https://psl.noaa.gov/data/gridded/>).

### 2.3. Identification of sea breeze days

For the analysis of sea breeze cooling capacity, sea breeze days should be firstly selected based on data from Adelaide Airport weather station. The basic concept of a sea breeze is that it starts after sunrise when the land is warmer than the nearby sea. In addition, wind direction in the coastal area is supposed to change from offshore to onshore during a sea breeze event. The sea breeze can also lead to changes in other meteorological variables, such as a decrease in air temperature and an increase in specific humidity. Therefore, we adopt six groups of screening criteria in identifying sea breeze days using data from Adelaide Airport weather station and other relevant data:

1. Wind rotates more than  $45^\circ$  within half an hour since the arrival of a sea breeze.
2. After the rotation of wind, wind direction stabilizes within  $180^\circ - 320^\circ$  ( $0^\circ$  from the north, clockwise) for more than 2 h.
3. Air temperature decreases for more than 1 h after the arrival of a sea breeze.
4. Specific humidity increases for more than 1 h after the arrival of a sea breeze.
5. The arrival time of a sea breeze is restricted within 6:00–16:00.
6. Land surface temperature is higher than the nearby sea surface temperature.

### 2.4. Sea breeze cooling capacity

After the selection of sea breeze days, we perform calculation and analysis of sea breeze cooling capacity based on data from the Adelaide urban heat island monitoring network. Sea breeze cooling capacity is a metric proposed to demonstrate the cooling ability of sea breezes. It is defined as the cumulative difference of temperature for the duration of a selected sea breeze day and an average of non-sea breeze days with adjusted air temperature to be that immediately before the arrival of the sea breeze.

In order to compare temperatures between sea breeze days and non-sea breeze days, we firstly define the reference temperature curve. It's the diurnal temperature cycle that is monthly averaged over non-sea breeze days when the diurnal temperature ranges are larger than a given threshold. The threshold is set to exclude other climatic effects (e.g., cloud, rain) as much as possible. In this study, it's set as  $6^\circ\text{C}$  according to the diurnal temperature ranges of sea breeze days in

Adelaide. For the calculation of SBCC, we also define the adjusted reference temperature curve as the curve adjusted from the reference temperature curve to match the observed temperature when cooling begins (usually in the morning). Therefore, SBCC can be considered as the difference between the adjusted reference temperature curve and the observed temperature curve:

$$\text{SBCC} = \text{REF} - \text{OBS} \quad (1)$$

where  $\text{REF}$  and  $\text{OBS}$  are time integrals of the adjusted reference temperature curve and the observed temperature curve during sea breeze cooling, respectively. The two curves can be calculated by Eq. (2) and Eq. (3) (Zhou et al., 2019):

$$\text{REF} = \sum_{i=2}^n \frac{(T_{\text{ref}(i-1)} + T_{\text{ref}(i)}) \times \Delta t}{2} \quad (2)$$

$$\text{OBS} = \sum_{i=2}^n \frac{(T_{\text{obs}(i-1)} + T_{\text{obs}(i)}) \times \Delta t}{2} \quad (3)$$

where  $T_{\text{ref}(i)}$  represents the value from the adjusted reference temperature curve at the time step of  $i$  and  $T_{\text{obs}(i)}$  represents the corresponding temperature from the observation.  $\Delta t$  is the time interval and  $n$  is the number of time steps. The unit of SBCC is  $^\circ\text{C h}$ .

The arrival time and retreat time of sea breeze cooling are based on temperature changes of the sea breeze day and they should be distinguished from previous definitions of arrival and retreat time of the sea breeze itself, which depend on wind conditions. Specifically, arrival time of sea breeze cooling is defined as the time when air temperature begins to decrease after sunrise, while the corresponding retreat time is the earliest of the following three time points: (1) the intercept of the adjusted reference temperature curve and the observed temperature curve, (2) the time offshore wind starts, or (3) a fixed time point of 23:00.

In addition to SBCC, we also use the index of maximum cooling ( $dT_{\text{max}}$ ) to investigate the intensity of cooling induced by sea breezes. It is defined as the maximum temperature difference between temperature observed and that on the adjusted reference curve for each sea breeze event.

### 2.5. Calculation of the distance from the coast

In order to analyze the penetration process of sea breeze cooling, we have calculated distances from the coast for individual sites along the prevailing wind path. Based on DEM data, we have firstly detected the coastline. For each site, the corresponding landing location of sea breeze cooling front can be identified as the intersection between the prevailing wind path for this site and coastline. Therefore, the distance from the coast is calculated as the length from this landing location to the corresponding site. In this study,  $225^\circ$  is set as the prevailing sea breeze direction (Zhou et al., 2019).

### 2.6. Jenkinson and Collison classification

The Jenkinson and Collison (hereafter, JC) classification is a widely used objective classification method in identifying synoptic types based on data of sea level pressure (Sarricolea et al., 2018). With this classification method, patterns of atmospheric circulations are revealed and therefore their relationships with sea breeze occurrences can be investigated. The JC method is designed to identify 27 synoptic types that can be classified into four groups: (1) anticyclonic (A) and cyclonic (C); (2) directional flows in eight wind directions (N; NE; E; SE; S; SW; W; NW); (3) hybrid types combining directional flows and cyclonic types (AN; ANE; AE; ASE; AS; ASW; AW; ANW; CN; CNE; CE; CSE; CS; CSW; CW; CNW); (4) the unclassified type (U). This method has been used in multiple fields such as analysis of atmospheric circulations, mechanism

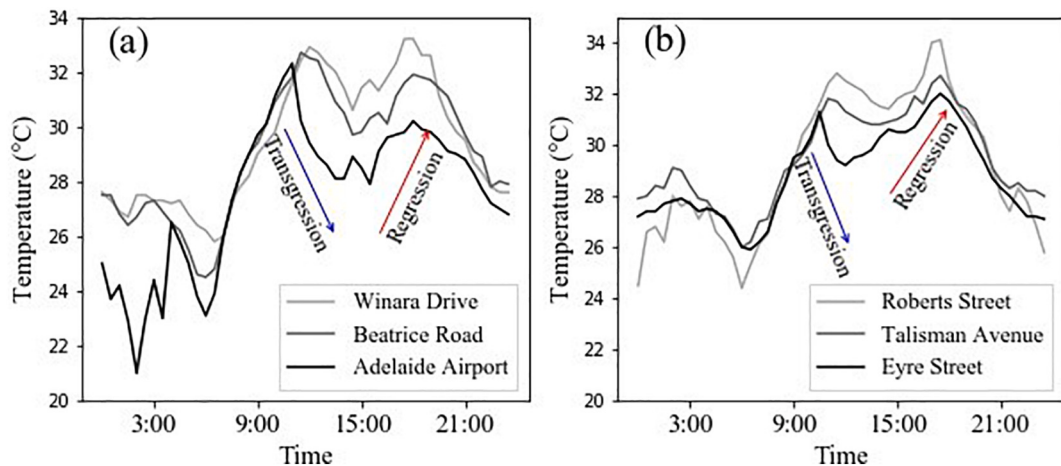


**Fig. 2.** Temperature patterns of a sea breeze day (6th, Mar, 2013) along the northern (a) and southern (b) transects of metropolitan Adelaide. For the northern transect, site 23 (Adelaide Airport), 39 (Beatrice Road) and 38 (Winara Drive) are selected, while for the southern transect, site 24 (Eyre Street), 25 (Talisman Avenue) and 34 (Roberts Street) are selected. The arrows on both subplots show the processes of transgression and regression of sea breeze cooling fronts.

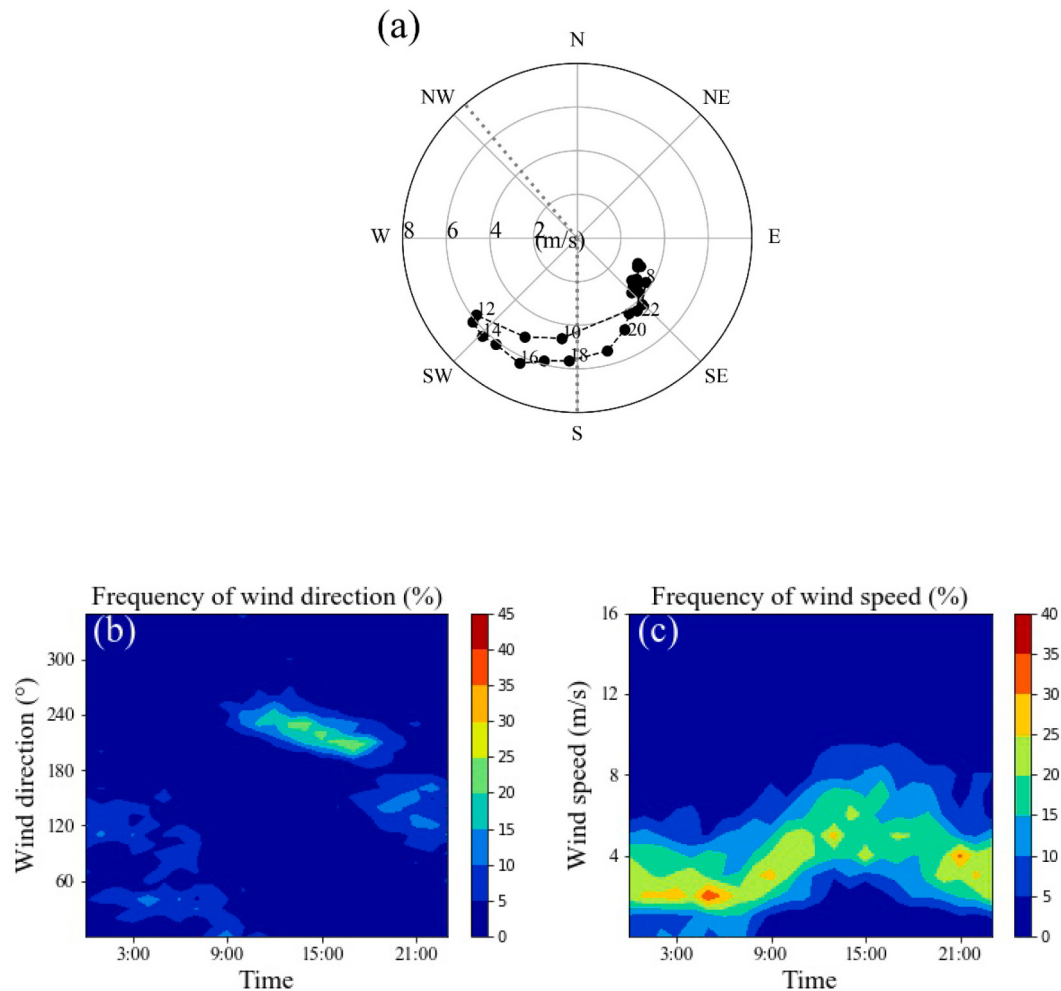


**Fig. 3.** (a) Wind hodograph averaged over sea breeze days. The two dotted lines represent the range of wind directions during sea breezes (180–320°). The values on the horizontal axis indicate wind speed and the values on the dashed line indicate time of the day (hours); (b) Pattern of hourly wind direction frequencies (%) during sea breeze days with an interval of 10°; (c) Pattern of hourly wind speed frequencies (%) during sea breeze days with an interval of 1 m/s.

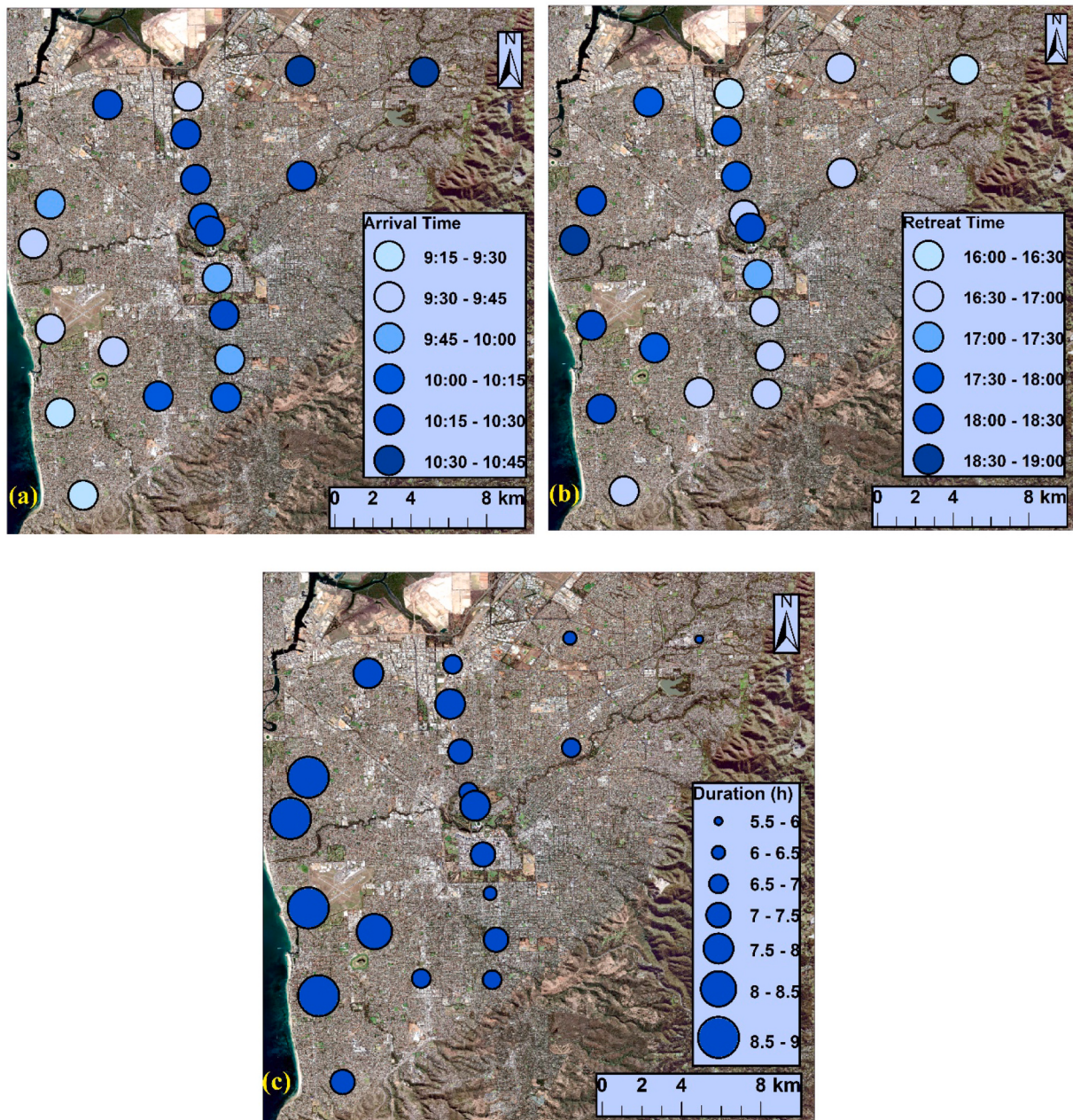


**Fig. 4.** Spatial patterns of arrival time (a), retreat time (b) and duration (c) of sea breeze cooling in metropolitan Adelaide averaged over all sea breeze events during summer days from December 2010 to March 2013.

of extreme events and synoptic background of sea breeze events (Broderick and Fealy, 2015; Pattison and Lane, 2012; Khan et al., 2018). In this study, we analyze the synoptic types during sea breeze days using the JC method to see how synoptic background influences sea breeze cooling. The analysis is based on NCEP/NCAR sea level pressure data of an area centered on Adelaide with 5° resolution in latitude and 10° resolution in longitude (25° - 45°S, 125° - 155°E).

### 3. Results and discussion

According to the criteria proposed above, we have identified 116 (31.9%) sea breeze days from 364 summer days during December 2010 – March 2013. This is consistent with findings in other parts of the world (Azorin-Molina et al., 2011; Shen et al., 2019). When compared with the sea breeze frequency of about 60% in Perth, which is located on the west coast of the Australian continent, this percentage is lower. A higher sea

breeze frequency in Perth is probably because of the West Coast Trough moving onshore on the west coast of Australia (Masselink and Pattiaratchi, 2001).

It is more interesting and relevant to examine sea breeze cooling during hot sea breeze days. In this study, hot sea breeze days are defined as sea breeze days with maximum temperatures above the 75th percentile of all sea breeze days (32.8 °C). Using this criterion, 29 days are identified as hot sea breeze days in Adelaide.

#### 3.1. Case study of a sea breeze event

In order to explain the spatial pattern of sea breeze cooling within metropolitan Adelaide, the diurnal patterns of air temperature at different sites are compared during an example of sea breeze day (6th, Mar, 2013). In this study, two transects are defined. Site 23 (Adelaide Airport), 39 (Beatrice Road) and 38 (Winara Drive) are selected as the

**Table 2**

Classification of sites based on distances from the coast along the prevailing wind path.

	Site number	The distance from the coast along the prevailing wind path
Group 1	23, 24, 25, 26, 27, 28, 29, 37	< 10 km
Group 2	3, 13, 14, 30, 31, 34, 36, 39	10–16 km
Group 3	32, 33, 35, 38	> 16 km

northern transect, while site 24 (Eyre Street), 25 (Talisman Avenue) and 34 (Roberts Street) are selected as the southern transect. The two transects are chosen because they are distributed along the prevailing wind path of sea breezes. The three sites along the northern transect are 2, 11 and 17 km from coast along the prevailing wind path, while the corresponding distances are 5, 9 and 11 km for the southern transect.

Diurnal changes of air temperature during this sea breeze day are shown in Fig. 2. The transgressions and regressions of cooling fronts along both transects are distinctly demonstrated. For the northern transect, all three sites experience significant temperature drops during the daytime. The earliest arrival of the cooling front appears at Adelaide Airport at about 11:30. With the penetration of the sea breeze inland, cooling is observed at Beatrice Road half an hour later and at Winara Drive one hour later. Correspondingly, the retreat time follows a reversed order. There are also clear gradients of maximum cooling and SBCC among the three sites. Specifically, SBCC values are 29.9 °C h, 15.6 °C h and 9.7 °C h, respectively. As for the three sites along the southern transect, the diurnal patterns of air temperature are similar and the corresponding SBCC values are 16.8 °C h, 10.8 °C h and 9.6 °C h, respectively. From the comparison between the two transects, we can see that the magnitude of the sea breeze cooling along the southern transect is significantly smaller than that along the northern transect with a similar distance from the coast. For example, SBCC at site 39 is 6 °C h larger than that at site 34 although both sites are about 11 km from coast.

### 3.2. Wind condition of sea breeze days

Wind direction and wind speed are major characteristics in explaining the dynamics of sea breezes. Therefore, we have analyzed the basic wind conditions during sea breezes based on data from Adelaide Airport station (anemometer at 10 m above ground). The hodograph in Fig. 3(a) shows the mean diurnal evolutions of both variables averaged over all sea breeze days. It is clear that there is a transition between

offshore and onshore wind. At 8:00 in the morning, there is a rapid shift in wind direction from southeast to southwest. In the afternoon, it returns to southeast until about 20:00 when winds start to stabilize. The average turning point is 233° at 12:00. It should be noted that winds mostly come from the south during sea breezes and this is different from cases in autumn and winter when northerly and westerly winds dominate. As for wind speed, it is mostly lighter than 4 m/s from 0:00 to 8:00. The wind speed gradually increases after sunrise to 6.3 m/s on average at 16:00. Overall, wind speed in the afternoon is higher than that in the morning. This agrees well with other sea breeze observations in mid-latitudes (Huang et al., 2016; Papanastasiou and Melas, 2009).

Wind pattern can also be further explained by the diurnal distribution of wind direction frequency during sea breeze days, which clearly demonstrates the contrast between daytime and nighttime. More than 68% of the winds blow within the range of 200–250° during 12:00–18:00, while a relatively higher percentage of wind directions between 0 and 180° occur during nighttime (Fig. 3(b)). As for wind speed, the magnitudes are much higher during 12:00–18:00. This is consistent with the time when wind directions are concentrated within 200–250° (Fig. 3(c)). The results demonstrate that sea breezes play important roles in influencing wind conditions in Adelaide.

### 3.3. Arrival time, retreat time and duration of sea breeze cooling

The arrival time and retreat time of a sea breeze cooling front are influenced by local topography and synoptic background (Ookouchi and Wakata, 1984; Estoqua, 1962), while the duration of sea breeze cooling (time span between its arrival and retreat) can indicate the cooling strength. These variables are estimated here based on the Adelaide urban heat island monitoring network for a better understanding of the basic characteristics of sea breeze climatology.

The mean arrival time of sea breeze cooling fronts in metropolitan Adelaide is shown in Fig. 4(a). A clear delaying pattern from coast to inland can be identified and site 24 (Eyre Street) is the site cooled the earliest by the sea breeze. Averaged over 116 sea breeze days, the cooling front arrival time is 9:29 am at this site. In contrast, the averaged arrival time is 10:36 at site 32 (Gorman Street), which is about 24 km from the coast along the prevailing wind path. This result demonstrates that it commonly takes more than one hour (67 min on average) for the sea breeze cooling front to penetrate over metropolitan Adelaide. In order to clearly compare the differences in key time points of a sea breeze cooling, we separate the sites into three groups based on their distances from the coast along the prevailing wind path. The detailed classification is demonstrated in Table 2. Arrival time, retreat time and duration classified by the three groups are shown in Fig. 5 in which the numerical distributions are calculated based on values averaged over all

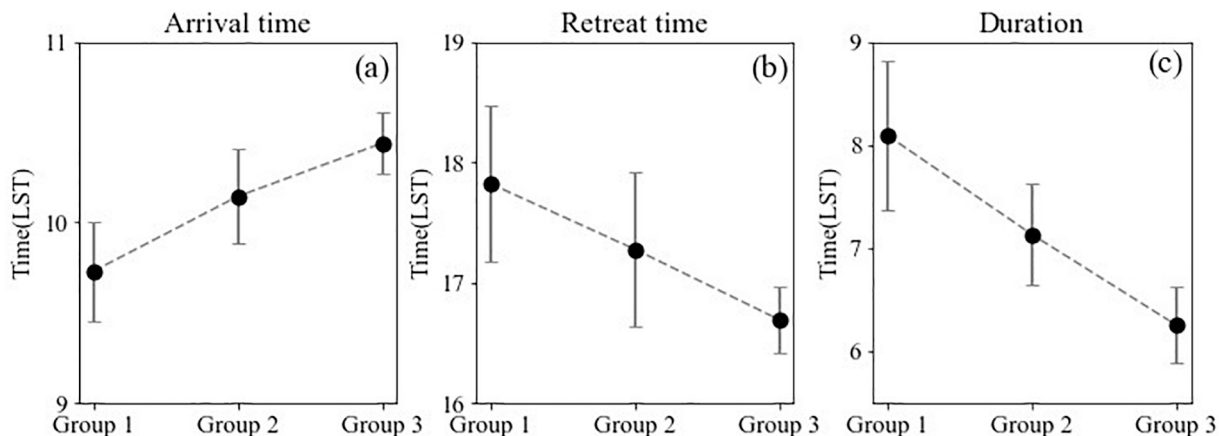
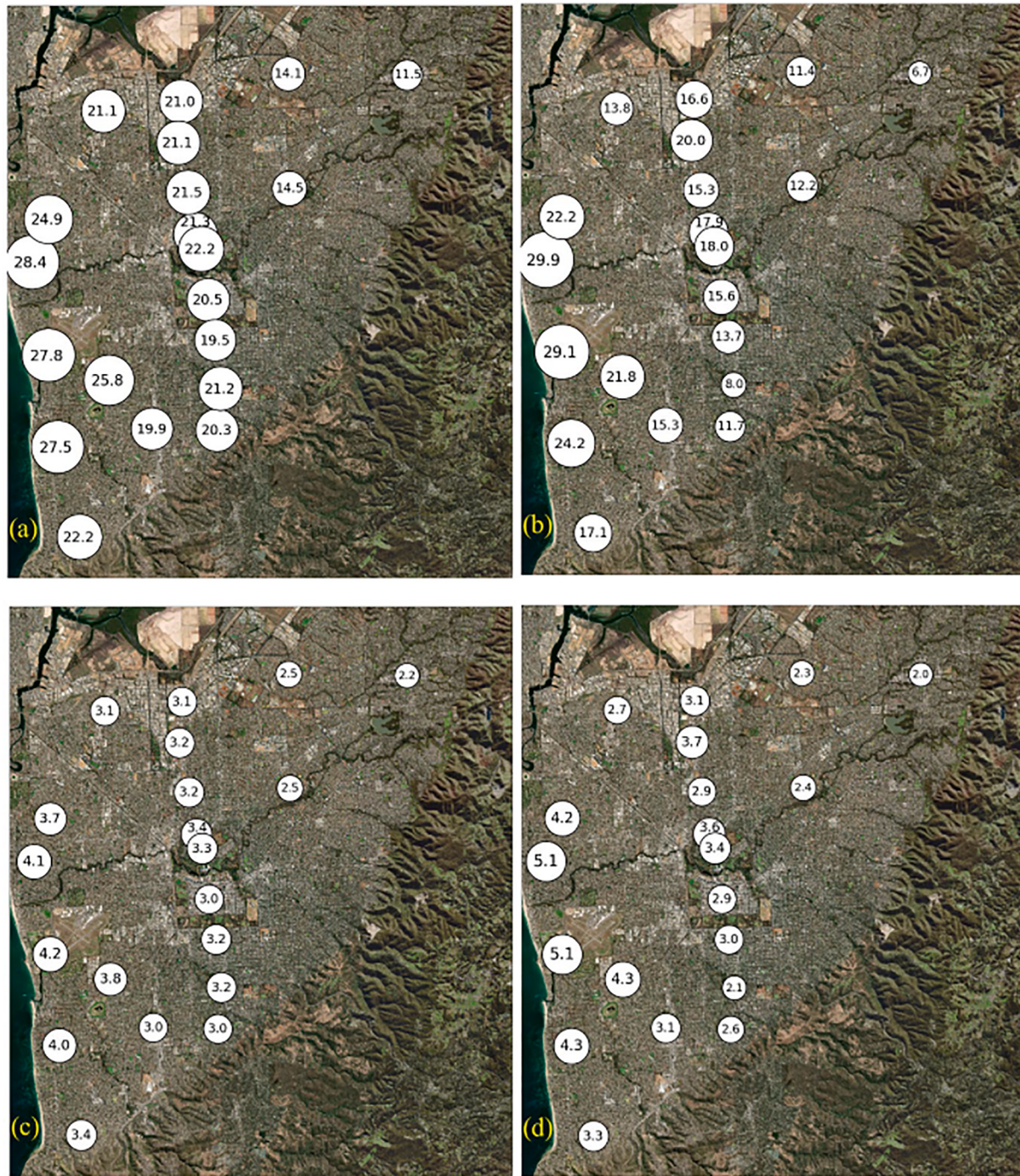


Fig. 5. Arrival time (a), retreat time (b) and duration (c) of sea breeze cooling classified by three groups based on distances from the coast along the prevailing wind path. The numerical distributions are calculated based on values averaged over all sea breeze days of individual sites.

sea breeze days of individual sites. From Fig. 5(a), the mean arrival time is 9:44, 10:09 and 10:26 for group 1, 2 and 3, respectively. This clearly shows the transgression of sea breezes.

Sea breeze cooling fronts normally retreat before sunset. Opposite to the spatial pattern of arrival time, retreats happen earlier at inland sites (Fig. 4(b)). On average, the earliest is found to be 16:14 (site 32), while the latest is 18:36 at a coastal site (site 27, Kent Avenue). This is not surprising as the sea breeze is weakened during the penetration inside the city and its cooling effect could disappear halfway when its intensity is discounted. For the three groups of sites, the mean values of corresponding retreat time are 17:49, 17:17 and 16:41, respectively (Fig. 5(b)).

Time durations of sea breeze cooling for individual sites have also been estimated based on arrival and retreat time of cooling fronts. The all-site mean duration is 7.3 h. There is a significantly decreasing trend from coast to inland ranging from 9.0 (site 27) to 5.6 (site 32) hours (Fig. 4(c)). For the three groups of sites, the mean durations are 8.1, 7.1 and 6.3 h, respectively (Fig. 5(c)). It can also be identified that durations of sea breeze cooling of the southernmost sites are shorter than other sites. More specifically, the mean daily duration of cooling is only 7.3 h at site 24 (Eyre Street), while the corresponding values are more than 8 h for other coastal sites.



**Fig. 6.** The spatial patterns of SBCC ( $^{\circ}\text{C h}$ ) (a,b) and  $\Delta\text{Tmax}$  ( $^{\circ}\text{C}$ ) (c,d) per event averaged from December 2010 to March 2013 in metropolitan Adelaide for all sea breeze days (a,c) and hot sea breeze days (b,d), respectively.

### 3.4. Sea breeze cooling capacity in metropolitan Adelaide during summer

The spatial patterns of calculated SBCC and maximum cooling ( $dT_{\max}$ ) in metropolitan Adelaide averaged over all sea breeze days and hot sea breeze days are presented in Fig. 6. The SBCC values range from 11.5 to 28.4 °C h per event (444.1–1098.1 °C h per season) during summer days and the spatial average is 21.3 °C h per event (824.5 °C h per season). As expected, the cooling power is evidently weakened from coast to inland mainly due to the roughness of urban surface and heat exchange of sea breezes with the local atmosphere. The largest cooling appears at site 27 (Kent Avenue). This site is only 2.2 km from the coast (Fig. 6(a)). Its surrounding area is relatively flat with only single-story residential housing. Therefore, sea breeze cooling at this site is less influenced by frictional effects from the urban surface. Similar magnitudes of SBCC appear at site 23 and 26, which are also near the coast.

Averaged over hot sea breeze days, there is also an inland decreasing pattern of SBCC with the largest one presented at site 27 and the smallest one at the most inland site (site 32, Gorman Street) (Fig. 6(b)). However, the corresponding SBCC values are apparently smaller in most sites when compared to other sea breeze days and the differences are gradually becoming larger from coast to inland. Therefore, the range across sites is larger from 6.7 to 29.9 °C h per event (64.3 – 289.4 °C h per season).

Similar spatial patterns and characteristics are also identified for  $dT_{\max}$  (Fig. 6(c), (d)). Averaged over all sea breeze days,  $dT_{\max}$  values are over 4 °C at Adelaide Airport and Kent Avenue, which are less than 2.5 km from coast. The values are even larger in hot sea breeze days (5.1 °C for both sites). However, when focusing on the inland sites, the magnitudes are smaller in hot sea breeze days than those in other sea breeze days, which further confirms the faster weakening rate during inland penetration under heatwave conditions. Linearly interpolated, the decreasing rates of  $dT_{\max}$  values along the prevailing wind path are 0.08 °C/km and 0.13 °C/km over all sea breeze days and hot sea breeze days, respectively.

In previous studies, there is no quantitative analysis of temperature reduction during sea breezes. However, similar gradients of air temperature at specific time points have been revealed in some studies. For example, in metropolitan Tokyo, there is a temperature difference of about 4 °C between the coastal area and Kawagoe which is 40 km inland during a sea breeze event (Yamato et al., 2017). The transgression relies on the local topography and the background synoptic system. Therefore, similar studies in other places are important for a better understanding of the effect of sea breeze cooling on heat mitigation with different topographical and climatic settings in future work.

Consistent with the spatial pattern of cooling duration discussed in Sect. 3.3, the magnitudes of sea breeze cooling are evidently smaller at the southernmost sites than the sites of similar distances from the coast in the north. This phenomenon is more pronounced in the coastal area. Averaged over all sea breeze days, SBCC is only 22.2 °C h per event at site 24 (Eyre Street), while the corresponding values are mostly larger than 27 °C h at other coastal sites (site 23: 27.8 °C h; site 26: 27.5 °C h; site 27: 28.4 °C h). In southern Adelaide, elevation along the prevailing wind path is higher than that in other parts of Adelaide. The complicated topography in southern Adelaide is likely to explain this lower cooling capacity.

### 3.5. Inland penetration distance of sea breeze cooling in metropolitan Adelaide

Because SBCC values are negatively related to distances from the coast in metropolitan Adelaide, the penetration distance of the cooling front can be calculated based on the location where SBCC drops to zero from this spatial relation. In this study, linear regression (better than higher order polynomial fits based on the Bayesian information criterion) between SBCC and the distance from the coast, is adopted to describe the sea breeze cooling penetration (Fig. 7). It demonstrates that

the weakening rate of SBCC values during the penetration is 0.7 °C h/km per event averaged over all sea breeze days. Based on this rate, the estimated penetration distance of cooling front along the prevailing wind path is 42 km without the consideration of variability in surface roughness. Consistent with the larger range in spatial SBCC, the attenuation rate is higher in hot sea breeze days being 0.9 °C h/km. The corresponding estimated penetration distance is 29 km. This means that the cooling effect covers nearly the whole metropolitan area of Adelaide.

Synoptic background is an important factor influencing the interaction between sea breezes and the local environment. In order to explore the mechanism leading to the higher attenuation rate of sea breeze cooling during hot sea breeze days, we analyze synoptic types during all sea breeze days and hot sea breeze days respectively based on JC classification method (Jenkinson and Collison, 1977). The corresponding distributions are shown in Fig. 8. For all sea breeze days, the most frequent type is anti-cyclone (A: 24 days, 20.7%), followed by three directional flows (E: 12 days, 10.3%; SE: 12 days, 10.3%; S: 14 days, 12.1%). However, more than 40% of hot sea breeze days experience eastern and southeastern directional flows (E: 7 days, 24.1%; SE: 6 days, 20.7%). Only one hot sea breeze day has an anti-cyclone pattern (3.4%). In addition, for hybrid types that combine directional flows and cyclonic/anti-cyclonic patterns, the directional components are also dominated by easterly patterns in hot sea breeze days.

In the southern hemisphere, the Coriolis Force moves the horizontal airflow towards the left, so the typical easterly and southeasterly synoptic patterns lead to northerly and north-easterly winds in Adelaide. In fact, a large area of dryland where the air temperature is extremely high in summer is located to the northeast of metropolitan Adelaide. Winds blowing from this area can contribute to high temperature in Adelaide and counteract the sea breeze cooling effect to a certain extent. Therefore, the large-scale synoptic patterns explain the faster weakening process of sea breeze cooling during hot sea breeze days.

The penetration distance of sea breeze cooling shown here is conceptually different from that of a sea breeze, although they are relevant. The latter has been investigated in the literature. Salvador and Millán (2003) have proposed a method using observed data (Azorin-Molina et al., 2011) to calculate the inland penetration distance of a sea

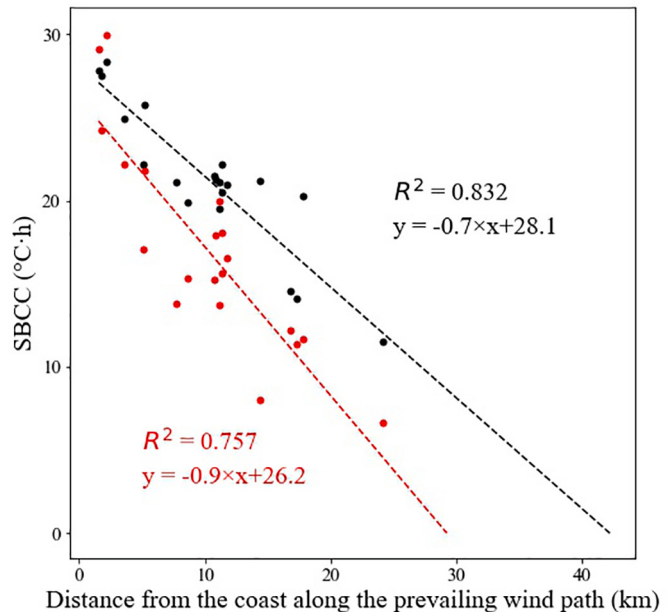


Fig. 7. The relationship between the distance from the coast along the prevailing wind path and SBCC averaged over all sea breeze days (black) and hot sea breeze days (red) from December 2010 to March 2013 for individual sites in metropolitan Adelaide.

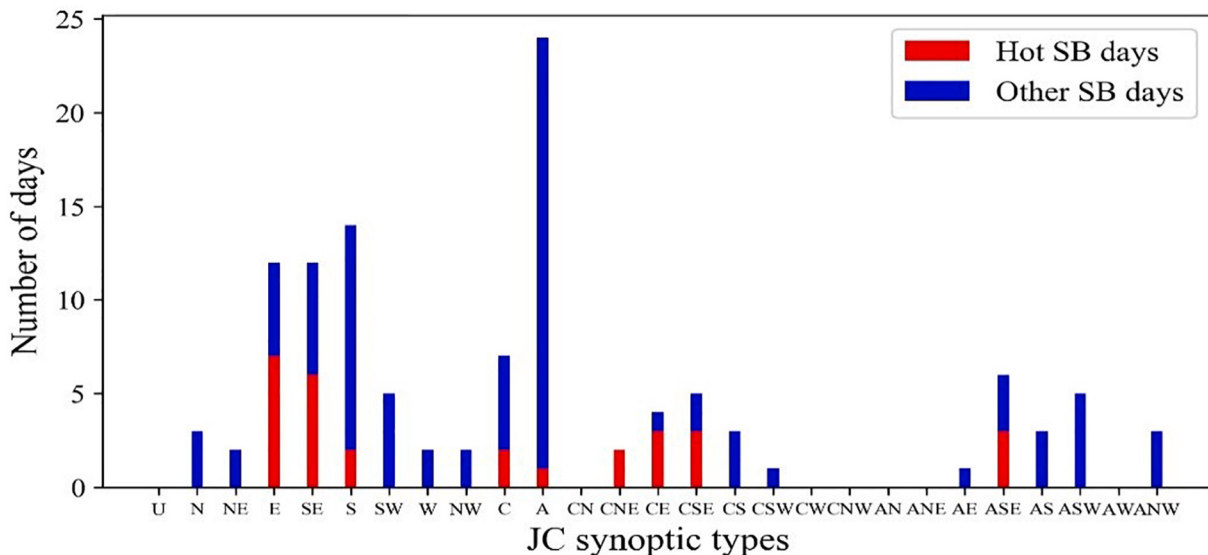


Fig. 8. Distribution of JC synoptic types during hot sea breeze days and other sea breeze days.

breeze. With this method, the sea-breeze penetration distance is calculated by multiplying a fixed wind speed and a specific time interval. This method has been widely used in studies on sea breezes with estimated sea-breeze penetration distances of up to 300 km (Khan et al., 2018). Salvador's method does not consider the weakening effect of the sea breeze during its inland penetration. Cloud-lines extracted from satellite observations have proven to identify sea breeze fronts well and this can be used in the analysis of sea breeze penetration (Hadi et al., 2002; Ferdiansyah et al., 2020). However, it should be noted that sea breezes interact with the underlying land cover, thus their properties (e.g., temperature) change during the penetration. In cities, high-rise buildings can contribute to the upwelling of low-level air and rapidly change temperature of the air mass (Allegrini and Carmeliet, 2017). Due to these interactions, the state of a sea breeze changes along its path. Therefore, the penetration distance of sea breeze cooling power is different from that of the sea breeze itself. Without using the measurements of air temperature throughout a coastal area, the estimated sea-breeze penetration distances from these methods do not represent the coverage area of sea breeze cooling.

It should be noted that 225° is set as the prevailing sea breeze direction in this study. In fact, this angle is a statistical value based on local weather condition during sea breeze days in Adelaide. In real condition, the prevailing wind path might vary slightly case by case. Therefore, potential uncertainties of the calculated distances from the coast exist.

### 3.6. Mapping SBCC in metropolitan Adelaide

As mentioned in Sect. 3.4, there is a clear decreasing pattern of SBCC values during the inland penetration of sea breeze cooling and the magnitudes of SBCC are supposed to be affected by terrain effects. A multiple linear regression of spatial SBCC per event with geographical variables is performed. In this study, elevation at the onshore point ( $Z$ ) and the distance from the coast along the prevailing wind path ( $D$ ) are utilized as independent variables. The former one is chosen because topography on the coast may impact sea breeze cooling. In this study, elevation at the onshore point is defined as the mean elevation of the corresponding coastal raster with 30-m width along the prevailing wind path of each site. The result demonstrates that both variables are statistically significant in explaining the spatial variability of SBCC with  $p$  values being 0.00 for the distance from the coast and 0.03 for elevation at the onshore point, respectively. With the increase of inland distance and elevation at the onshore point, there will be a smaller SBCC.

According to the regression result, the two variables together explain 87.6% of the spatial variability of the temporally average SBCC. This suggests that SBCC distribution in Adelaide can be estimated using this regression function:  $SBCC (\text{ }^{\circ}\text{C h}) = -0.7 \times D (\text{km}) - 0.3 \times Z (\text{m}) + 31.7$ .

## 4. Conclusions

The sea breeze has the potential to cool the local environment and therefore mitigate the urban heat in summer. In this study, we analyze sea breeze cooling capacity (SBCC) and propose a new method to estimate its inland penetration based on observed data from the Adelaide urban heat island monitoring network.

In the study period of 364 summer days from December 2010 to March 2013, we have identified 116 days as sea breeze days. During the process of sea breeze cooling, wind direction changes from southeast to southwest in the morning, and it gradually returns to southeast in the afternoon. Averaged over all sea breeze days, the cooling arrival time ranges from 9:29 to 10:36 for individual sites, while the corresponding retreat time ranges from 16:14 to 18:36. The SBCC value is 21.3 °C h per event averaged spatially in Adelaide summer. As for the spatial distribution of SBCC values, there is a decreasing pattern from coast to inland. Averaged over hot sea breeze days, SBCC values are particularly smaller in most of the sites and the differences are gradually getting larger from coast to inland.

Based on the negative relationship between SBCC values and distances from the coast, a new method for estimating the penetration distance of sea breeze cooling has been proposed and applied. Using this method, the penetration distance of sea breeze cooling is estimated to be about 42 km along the prevailing wind path (225°). For hot sea breeze days, the corresponding distance declines to about 29 km. With the analysis of Jenkinson and Collison (JC) synoptic types in hot sea breeze days and other sea breeze days, it has been found that the large-scale synoptic patterns can explain this phenomenon. In addition, the result from multiple linear regression shows that the distance from the coast along the prevailing wind path (225°) and elevation at the onshore point together explain 87.6% of the spatial variability of the temporally average SBCC in the study area.

## Declaration of Competing Interest

None.

## Acknowledgement

Government of South Australia, Adelaide City Council, Goyder Institute for Water Research, and South Australia Water Corporation provided funding for the Adelaide urban heat island monitoring network, on which this study was based. Vinokumar, John Bennett, Cecilia Ewenz, and Chris Kent contributed to data collection. The first author is supported by China Scholarship Council for his PhD study. Other data were obtained from Bureau of Meteorology, Australia, and NOAA, USA. Constructive comments from Roger Clay and two reviewers are appreciated.

## References

- Ado, H.Y., 1992. Numerical study of the daytime urban effect and its interaction with the sea breeze. *J. Appl. Meteorol.* 31 (10), 1146–1164.
- Allegri, J., Carmeliet, J., 2017. Coupled CFD and building energy simulations for studying the impacts of building height topology and buoyancy on local urban microclimates. *Urban Clim.* 21, 278–305. <https://doi.org/10.1016/j.ulclim.2017.07.005>.
- Arrillaga, J.A., Yagüe, C., Sastre, M., Román-Cascón, C., 2016. A characterisation of sea-breeze events in the eastern Cantabrian coast (Spain) from observational data and WRF simulations. *Atmos. Res.* 181, 265–280. <https://doi.org/10.1016/j.atmosres.2016.06.021>.
- Azorin-Molina, C., Chen, D., 2009. A climatological study of the influence of synoptic-scale flows on sea breeze evolution in the Bay of Alicante (Spain). *Theor. Appl. Climatol.* 96 (3–4), 249–260. <https://doi.org/10.1007/s00704-008-0028-2>.
- Azorin-Molina, C., Chen, D., Tijm, S., Baldi, M., 2011. A multi-year study of sea breezes in a Mediterranean coastal site: Alicante (Spain). *Int. J. Climatol.* 31 (3), 468–486. <https://doi.org/10.1002/joc.2064>.
- Bastin, S., Drobinski, P., Dabas, A., Delville, P., Reitebuch, O., Werner, C., 2005. Impact of the Rhône and Durance valleys on sea-breeze circulation in the Marseille area. *Atmos. Res.* 74 (1–4), 303–328. <https://doi.org/10.1016/j.atmosres.2004.04.014>.
- Broderick, C., Fealy, R., 2015. An analysis of the synoptic and climatological applicability of circulation type classifications for Ireland. *Int. J. Climatol.* 35 (4), 481–505. <https://doi.org/10.1002/joc.3996>.
- Chen, F., Miao, S., Tewari, M., Bao, J.W., Kusaka, H., 2011. A numerical study of interactions between surface forcing and sea breeze circulations and their effects on stagnation in the greater Houston area. *J. Geophys. Res.-Atmos.* 116 (D12) <https://doi.org/10.1029/2010JD015533>.
- Clay, R., Guan, H., 2020. The urban-parkland nocturnal temperature interface. *Urban Clim.* 31, 100585. <https://doi.org/10.1016/j.ulclim.2020.100585>.
- Coumou, D., Rahmstorf, S., 2012. A decade of weather extremes. *Nat. Clim. Chang.* 2 (7), 491–496. <https://doi.org/10.1038/nclimate1452>.
- Dandou, A., Tombrou, M., Soulakellis, N., 2009. The influence of the city of Athens on the evolution of the sea-breeze front. *Bound.-Layer Meteorol.* 131 (1), 35–51. <https://doi.org/10.1007/s10546-008-9306-x>.
- Estoque, M.A., 1962. The sea breeze as a function of the prevailing synoptic situation. *J. Atmos. Sci.* 19 (3), 244–250.
- Ferdiansyah, M.R., Inagaki, A., Kanda, M., 2020. Detection of sea-breeze inland penetration in the coastal-urban region using geostationary satellite images. *Urban Clim.* 31, 100586. <https://doi.org/10.1016/j.ulclim.2020.100586>.
- Freitas, E.D., Rozoff, C.M., Cotton, W.R., Dias, P.L.S., 2007. Interactions of an urban heat island and sea-breeze circulations during winter over the metropolitan area of São Paulo, Brazil. *Bound.-Layer Meteorol.* 122 (1), 43–65. <https://doi.org/10.1007/s10546-006-9091-3>.
- Furberg, M., Steyn, D.G., Baldi, M., 2002. The climatology of sea breezes on Sardinia. *Int. J. Climatol.* 22 (8), 917–932. <https://doi.org/10.1002/joc.780>.
- Guan, H., McGrath, A.J., Clay, R., Ewenz, C., Benger, S., Bennett, J., 2015. Effective surface areas for optimal correlations between surface brightness and air temperatures in an urban environment. *J. Appl. Remote. Sens.* 9 (1), 096059. <https://doi.org/10.1117/1.JRS.9.096059>.
- Guan, H., Kumar, V., Clay, R., Kent, C., Bennett, J., Ewenz, C., Simmons, C.T., 2016. Temporal and spatial patterns of air temperature in a coastal city with a slope base setting. *J. Geophys. Res.-Atmos.* 121 (10), 5336–5355. <https://doi.org/10.1002/2016JD025139>.
- Hadi, T.W., Horinouchi, T., Tsuda, T., Hashiguchi, H., Fukao, S., 2002. Sea-breeze circulation over Jakarta, Indonesia: a climatology based on boundary layer radar observations. *Mon. Weather Rev.* 130 (9), 2153–2166.
- He, B.J., 2018. Potentials of meteorological characteristics and synoptic conditions to mitigate urban heat island effects. *Urban Clim.* 24, 26–33. <https://doi.org/10.1016/j.ulclim.2018.01.004>.
- He, B.J., Ding, L., Prasad, D., 2020. Outdoor thermal environment of an open space under sea breeze: A mobile experience in a coastal city of Sydney, Australia. *Urban Clim.* 31, 100567. <https://doi.org/10.1016/j.ulclim.2019.10.057>.
- Huang, M., Gao, Z., Miao, S., Xu, X., 2016. Characteristics of sea breezes over the Jiangsu coastal area, China. *Int. J. Climatol.* 36 (12), 3908–3916. <https://doi.org/10.1002/joc.4602>.
- Jenkinson, A.F., Collison, F.P., 1977. An initial climatology of gales over the North Sea. *Synoptic Climatol. Branch Memorandum* 62, 18.
- Kala, J., Lyons, T.J., Abbs, D.J., Nair, U.S., 2010. Numerical simulations of the impacts of land-cover change on a southern sea breeze in south-West Western Australia. *Bound.-Layer Meteorol.* 135 (3), 485–503. <https://doi.org/10.1007/s10546-010-9486-z>.
- Khan, S.M., Simpson, R.W., 2001. Effect of a heat island on the meteorology of a complex urban airshed. *Bound.-Layer Meteorol.* 100 (3), 487–506. <https://doi.org/10.1023/A:1019284332306>.
- Khan, B., Abuallaja, Y., Al-Subhi, A.M., Nellayaputhenpeedika, M., Nelliakkattu Thody, M., Sturman, A.P., 2018. Climatology of sea breezes along the Red Sea coast of Saudi Arabia. *Int. J. Climatol.* 38 (9), 3633–3650. <https://doi.org/10.1002/joc.5523>.
- Kim, Y.H., Baik, J.J., 2004. Daily maximum urban heat island intensity in large cities of Korea. *Theor. Appl. Climatol.* 79 (3–4), 151–164. <https://doi.org/10.1007/s00704-004-0070-7>.
- Lapola, D.M., Braga, D.R., Di Giulio, G.M., Torres, R.R., Vasconcellos, M.P., 2019. Heat stress vulnerability and risk at the (super) local scale in six Brazilian capitals. *Clim. Chang.* 154 (3–4), 477–492. <https://doi.org/10.1007/s10584-019-02459-w>.
- Lopes, A., Lopes, S., Matzarakis, A., Alcoforado, M.J., 2011. The influence of the summer sea breeze on thermal comfort in Funchal (Madeira). A contribution to tourism and urban planning. *Meteorol. Z.* 20 (5), 553–564. <https://doi.org/10.1127/0941-2948/2011/0248>.
- Masouleh, Z.P., 2015. Identification of Sea Breezes, their Climatic Trends and Causation, with Application to the Adelaide Coast.
- Masselink, G., Pattiarratchi, C.B., 2001. Characteristics of the sea breeze system in Perth, Western Australia, and its effect on the nearshore wave climate. *J. Coast. Res.* 173–187.
- Meir, T., Orton, P.M., Pullen, J., Holt, T., Thompson, W.T., Arend, M.F., 2013. Forecasting the New York City urban heat island and sea breeze during extreme heat events. *Weather Forecast.* 28 (6), 1460–1477.
- Miller, S.T.K., Keim, B.D., Talbot, R.W., Mao, H., 2003. Sea breeze: Structure, forecasting, and impacts. *Rev. Geophys.* 41 (3) <https://doi.org/10.1029/2003RG000124>.
- Naor, R., Potchter, O., Shafir, H., Alpert, P., 2017. An observational study of the summer Mediterranean Sea breeze front penetration into the complex topography of the Jordan Rift Valley. *Theor. Appl. Climatol.* 127 (1–2), 275–284.
- Neumann, J., 1951. Land breezes and nocturnal thunderstorms. *J. Meteorol.* 8 (1), 60–67. [https://doi.org/10.1175/1520-0469\(1951\)008<0060:LBANT>2.0.CO;2](https://doi.org/10.1175/1520-0469(1951)008<0060:LBANT>2.0.CO;2).
- Ohashi, Y., Kida, H., 2002. Local circulations developed in the vicinity of both coastal and inland urban areas: a numerical study with a mesoscale atmospheric model. *J. Appl. Meteorol.* 41 (1), 30–45.
- Ookouchi, Y., Wakata, Y., 1984. Numerical simulation for the topographical effect on the sea-land breeze in the Kyushu island. *J. Meteorol. Soc. Japan. Ser. II* 62 (6), 864–879. <https://doi.org/10.2151/jmsj1965.62.6.864>.
- Papanastasiou, D.K., Melas, D., 2009. Climatology and impact on air quality of sea breeze in an urban coastal environment. *Int. J. Climatol.* 29 (2), 305–315. <https://doi.org/10.1002/joc.1707>.
- Pattiarratchi, C., Gould, B.H.J., 1997. Impact of sea-breeze activity on nearshore and foreshore processes in. *Cont. Shelf Res.* 17 (13), 1539–1560.
- Pattison, I., Lane, S.N., 2012. The relationship between Lamb weather types and long-term changes in flood frequency, River Eden, UK. *Int. J. Climatol.* 32 (13), 1971–1989. <https://doi.org/10.1002/joc.2415>.
- Poljak, G., Prtenjak, M.T., Kvakić, M., Strelec Mahović, N., Babić, K., 2014. Wind patterns associated with the development of daytime thunderstorms over Istria. *Ann. Geophys.* 32, 401–420. <https://doi.org/10.5194/angeo-32-401-2014>.
- Razzaghmanesh, M., Beecham, S., Salemi, T., 2016. The role of green roofs in mitigating Urban Heat Island effects in the metropolitan area of Adelaide, South Australia. *Urban For. Urban Green.* 15, 89–102. <https://doi.org/10.1016/j.ufug.2015.11.013>.
- Ribeiro, F.N., de Oliveira, A.P., Soares, J., de Miranda, R.M., Barlage, M., Chen, F., 2018. Effect of sea breeze propagation on the urban boundary layer of the metropolitan region of São Paulo, Brazil. *Atmos. Res.* 214, 174–188. <https://doi.org/10.1016/j.atmosres.2018.07.015>.
- Salvador, R.O.S.A., Millán, M., 2003. Análisis histórico de las brisas en Castellón. *Tethys* 2, 37–51.
- Sarricolea, P., Meseguer-Ruiz, O., Martín-Vide, J., Outeiro, L., 2018. Trends in the frequency of synoptic types in Central-Southern Chile in the period 1961–2012 using the Jenkinson and Collison synoptic classification. *Theor. Appl. Climatol.* 134 (1–2), 193–204. <https://doi.org/10.1007/s00704-017-2268-5>.
- Sasaki, Y., Matsuo, K., Yokoyama, M., Sasaki, M., Tanaka, T., Sadohara, S., 2018. Sea breeze effect mapping for mitigating summer urban warming: for making urban environmental climate map of Yokohama and its surrounding area. *Urban Clim.* 24, 529–550. <https://doi.org/10.1016/j.ulclim.2017.07.003>.
- Shen, L., Zhao, C., 2020. Dominance of Shortwave Radiative heating in the Sea-Land Breeze Amplitude and its Impacts on Atmospheric Visibility in Tokyo, Japan. *J. Geophys. Res.-Atmos.* 125 (8) <https://doi.org/10.1029/2019JD031541>.
- Shen, L., Zhao, C., Ma, Z., Li, Z., Li, J., Wang, K., 2019. Observed decrease of summer sea-land breeze in Shanghai from 1994 to 2014 and its association with urbanization. *Atmos. Res.* 227, 198–209. <https://doi.org/10.1016/j.atmosres.2019.05.007>.
- Smoyer-Tomic, K.E., Kuhn, R., Hudson, A., 2003. Heat wave hazards: an overview of heat wave impacts in Canada. *Nat. Hazards* 28 (2–3), 465–486. <https://doi.org/10.1023/A:1022946528157>.
- Suppiyah, R., Preston, B., Whetton, P.H., McInnes, K.L., Jones, R.N., Macadam, I., Kirono, D., 2006. Climate change under enhanced greenhouse conditions in South Australia. In: Climate Impacts and Risk Group. CSIRO Marine and Atmospheric Research, Melbourne.
- Trewin, B., Vermont, H., 2010. Changes in the frequency of record temperatures in Australia, 1957–2009. *Aust Meteorol. Oceanogr. J.* 60, 113–119.

- Wang, S., Zhu, J., 2020. Amplified or exaggerated changes in perceived temperature extremes under global warming. *Clim. Dyn.* 54 (1–2), 117–127. <https://doi.org/10.1007/s00382-019-04994-9>.
- Yamamoto, Y., Ishikawa, H., 2020. Influence of urban spatial configuration and sea breeze on land surface temperature on summer clear-sky days. *Urban Clim.* 31, 100578 <https://doi.org/10.1016/j.uclim.2019.100578>.
- Yamato, H., Mikami, T., Takahashi, H., 2017. Impact of sea breeze penetration over urban areas on midsummer temperature distributions in the Tokyo Metropolitan area. *Int. J. Climatol.* 37 (15), 5154–5169. <https://doi.org/10.1002/joc.5152>.
- Zhang, K., Zhao, C., Fan, H., Yang, Y., Sun, Y., 2019. Toward understanding the differences of PM 2.5 characteristics among five China Urban Cities. *Asia-Pac. J. Atmos. Sci.* 1–10. <https://doi.org/10.1007/s13143-019-00125-w>.
- Zhou, Y., Guan, H., Huang, C., Fan, L., Gharib, S., Batelaan, O., Simmons, C., 2019. Sea breeze cooling capacity and its influencing factors in a coastal city. *Build. Environ.* 166, 106408 <https://doi.org/10.1016/j.buildenv.2019.106408>.